Exposing the dead-cone effect of jet quenching in QCD medium*

Yun-Fan Liu (刘云帆)[1] Wei Dai (代巍)[1†] Ben-Wei Zhang (张本威)[2,3‡] Enke Wang (王恩科)[2,3,4]

[1]School of Mathematics and Physics, China University of Geosciences, Wuhan 430074, China
[2]Key Laboratory of Quark & Lepton Physics (MOE) and Institute of Particle Physics, Central China Normal University, Wuhan 430079, China
[3]Guangdong Provincial Key Laboratory of Nuclear Science, Institute of Quantum Matter, South China Normal University, Guangzhou 510006, China
[4]Guangdong-Hong Kong Joint Laboratory of Quantum Matter, Southern Nuclear Science Computing Center, South China Normal University, Guangzhou 510006, China

Abstract: When an energetic parton traverses the hot QCD medium, it may suffer from multiple scattering and lose its energy. The medium-induced gluon radiation for a massive quark will be suppressed relative to that of a light quark due to the dead-cone effect. The development of new declustering techniques of jet evolution makes a direct study of the dead-cone effect in the QCD medium possible for the first time. In this work, we compute the emission angle distribution of the charm-quark-initiated splittings in D^0 meson tagged jet and that of the light parton-initiated splittings in an inclusive jet in p+p and Pb+Pb at 5.02 TeV by utilizing the declustering techniques of jet evolution. The heavy quark propagation and induced energy loss in the QCD medium are simulated with the SHELL model based on the Langevin equation. By directly comparing the emission angle distributions of charm-quark-initiated splittings with those of light parton-initiated splittings at the same energy intervals of the initial parton, we provide insights into the fundamental splitting structure in A+A collisions, thereby exploring the possible observation of the dead-cone effect in medium-induced radiation. We further investigate the case of the emission angle distributions normalized to the number of splittings and find the dead-cone effect will broaden the emission angle of the splitting and reduce the possibility for such splitting to occur, leading the massive parton to lose less energy. We also find that the collisional energy loss mechanism has a negligible impact on the medium modification to the emission angle distribution of the charm-quark-initiated splittings for D^0 meson-tagged jets.

Keywords: jet quenching, dead cone, jets, heavy ion

DOI: 10.1088/1674-1137/ada7cf **CSTR:** 32044.14.ChinesePhysicsC.49044108

I. INTRODUCTION

In Quantum Chromodynamics (QCD), the vacuum induces a fast parton emitting gluon in a process that can be described as a parton shower. The parton shower evolves into a multi-parton final state and then harmonizes into a cluster of final state hadrons in a similar direction, which can be detected and recognized as jets [1]. It has been observed in particle colliders that the fast parton can be produced in the initial hard scatterings with large momentum transfer, make subsequent emissions resulting in additional productions of quarks and gluons, and then be reconstructed as jets in the final state.

One can expect the radiation from a parton of mass (M) and energy (E) will be suppressed within an angular size of M/E. Such a phenomenon was named as the dead-cone effect [2], which manifested itself indirectly in various heavy flavor-related observables in particle collider experiments [3−6]. An iterative jet declustering technique [7−9] has emerged to help expose the jet substructure to the most basic splitting structure experimentally. The ALICE report [10] suggested a comparison between the emission angle distribution of charm-quark-initiated splittings in D^0 meson-tagged jets and that of light parton-initiated splittings in inclusive jets produced in p+p collision at 13 TeV at the proper radiator's energy intervals. Thus, one can directly observe the dead-cone effect of the charm quark for the first time.

In high-energy nuclear-nuclear collisions, the fast parton produced in the initial hard scattering may pass

Received 24 September 2024; Accepted 7 January 2025; Published online 8 January 2025

* Supported by the Major Project of Basic and Applied Basic Research of Guangdong Province, China (2020B0301030008), and the Natural Science Foundation of China (1935007, 11805167)

† E-mail: weidai@cug.edu.cn

‡ E-mail: bwzhang@mail.ccnu.edu.cn

through the de-confined state of quark-gluon plasma (QGP). The medium modification of the fast parton is referred to as the jet quenching phenomenon [11−15], which has been intensively studied theoretically and experimentally. One of the key mechanisms of jet quenching is thought to be the radiation of soft gluons induced by the scattering of the fast parton with the medium constituents [16−25]. Such in-medium emission is also predicted to suffer the dead-cone effect, which means that the medium-induced radiation probability of the fast parton traversing the hot medium is also suppressed within an angular size of M/E [18, 26−28]. This may result in several observations that are explained by the scenario of the heavy flavor quarks losing less energy than light flavor quarks in experimental measurements [29−33]. However, the dead-cone effect itself cannot be isolated and observed through these measurements. In p+p collisions, iterative declustering techniques have allowed exposure of the dead-cone effect. The application of such techniques to jets in heavy ion collisions might allow us to expose the dead-cone effect in medium-induced radiation and to understand the mass dependency of jet quenching. In this paper, we calculate the emission angle distribution of the charm-quark-initiated in-medium splittings in D^0meson-tagged jets and that of the light parton-initiated in-medium splittings in inclusive jets in Pb+Pb collisions at $\sqrt{s} = 5.02$ TeV. Moreover, we aim to expose the dead-cone effect of medium-induced radiation in jet quenching.

II. SPLITTING ANGLE DISTRIBUTIONS IN D^0 MESON-TAGGED JETS IN P+P

In this section, we reproduce the exact ALICE setup and observable in pp collisions to validate our vacuum reference. The observable is defined as

$$R(\theta) = \frac{1}{N^{D^0\text{jets}}} \frac{\mathrm{d}n^{D^0\text{jets}}}{\mathrm{d}\ln(1/\theta)} \Big/ \frac{1}{N^{\text{inclusive jet}}} \frac{\mathrm{d}n^{\text{inclusive jet}}}{\mathrm{d}\ln(1/\theta)}, \quad (1)$$

where the numerator represents the splitting angle distributions of charm-quark-initiated splittings for D^0 meson-tagged jets normalized to the number of jets, and the denominator represents the splitting angle distributions for inclusive jets also normalized to the number of jets. The ratio is taken for the same initial energy E_{Radiator} intervals. The non-dead-cone limit of such observables can be derived from calculating the splitting angle distribution in pure light-initiated jets from event generators and then replacing the numerator in Eq. (1) to be $(1/N^{\text{lightjets}})(\mathrm{d}n^{\text{lightjets}}/\mathrm{d}\ln(1/\theta))$.

PYTHIA 8 [34] is used as the event generator, and the anti-k_T algorithm [35] from the Fastjet package [36] is used to simulate the production of jets with a transverse momentum in the interval of $5 < p_{T,\text{jet}}^{\text{ch}} < 50$ GeV. The D^0-meson is selected in the transverse momentum interval $2 < p_T^{D^0} < 36$ GeV/c. Once the required jets are selected, the internal splitting tree is reconstructed. After the preparation of the jets, in the iterative de-clustering processes, the Cambridge-Aachen (C/A) algorithm [37] is implemented to recluster the constituents in jets using the angular-ordered nature of the splittings, as in the QCD emissions. By iterative declustering of the splitting tree, the reclustering history is exposed. The measurements of the primary two-prong structures are recorded at each declustering step: the angle between the daughter prongs in splittings, θ, the relative momentum transfer of the splitting, k_T, and the energy of the parton initiating the splitting (the radiator), E_{Radiator}. $k_T > \Lambda_{\text{QCD}} = 200$ MeV/c is implemented to suppress the hadronisation effects [38]. The prongs containing D^0-mesons are always being followed to reconstruct the gluon emission history off a charm quark in a vacuum with an emission angle at each splitting process. The contaminations of gluon splitting contribution of the heavy flavor production were studied with MC simulations and found to be negligible. A minimum cut is imposed on the leading charged hadron in the leading prong of the recorded splitting in inclusive jets, $p_T^{\text{leadinghadron}} \geq 2.8$ GeV/s, which corresponds to the lower transverse momentum cut 2 GeV of the D^0-meson in D^0 meson-tagged jets.

In Fig. 1, we reproduce the ratios of splitting angle distributions $R(\theta)$ for D^0 meson-tagged jets (light-quark jets) to inclusive jets in p+p collisions at $\sqrt{s} = 13$ TeV using PYTHIA 8. The results are demonstrated for three energy intervals of the radiators: $5 < E_{\text{Radiator}} < 10$ GeV (left panel), $10 < E_{\text{Radiator}} < 20$ GeV (middle panel), and $20 < E_{\text{Radiator}} < 35$ GeV (right panel), which is the same as in Ref. [10], to compare with ALICE data. In these comparisons, PYTHIA 8 is proven to be sufficient to fairly describe the differences between the heavy and light quark-initiated splitting angular distributions within a jet along with the analysis procedures mentioned above. The observable $R(\theta)$ can help demonstrate the differences of the radiation angular distributions of a charm quark and light quarks, further exposing the dead-cone effect of charm quark by illustrating suppression in the $\ln(1/\theta)$ regions, which are colored in each E_{Radiator} interval. These colored areas correspond to the dead-cone angles in each interval, $\theta_{\text{dc}} < m_c/E_{\text{Radiator}}$. With an increase in E_{Radiator}, we can observe that the suppression in the lower θ region is weaker because the dead-cone region of θ is smaller.

When understanding the "suppression", theoretically, $R(\theta)$ cannot compare with unity because$N^{D^0\text{jets}}$ and $N^{\text{inclusive jet}}$ will not be the same, and the denominator of such a ratio that is used to compare the θ distributions in D^0 meson-tagged jets are reconstructed from inclusive jets in which there are light-quark- and gluon-initiated splittings involved. Still, the advantage of such an observ-

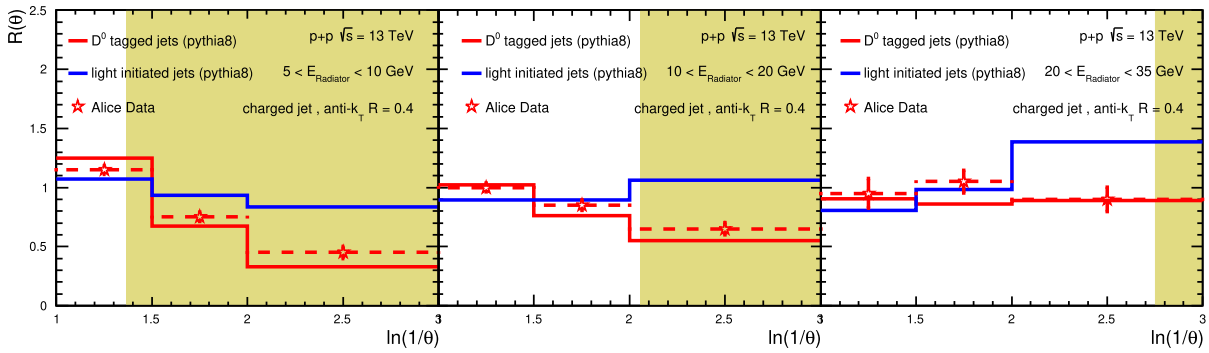

Fig. 1. (color online) Ratios of splitting angle distributions for D^0 meson-tagged jets (light-quark jets) to inclusive jets, $R(\theta)$ in p+p collisions at $\sqrt{s} = 13$ TeV using PYTHIA 8. The results are demonstrated for three energy intervals of the radiators: $5 < E_{\rm Radiator} < 10$ GeV (left panel), $10 < E_{\rm Radiator} < 20$ GeV (middle panel), and $20 < E_{\rm Radiator} < 35$ GeV (right panel), and they are compared with ALICE experimental data. The shaded areas correspond to the angles in which the radiation is suppressed due to the dead-cone effect, and the mass of the charm quark is assumed to be 1.275 GeV/c^2.

able is that it is experimentally measurable and still decisively manifests suppression in the dead-cone region of θ. Moreover, the plots with no dead-cone limits are also plotted accordingly. The deviations between the $R(\theta)$ curve of D^0 meson-tagged jets and no dead-cone limit are much more pronounced.

III. THEORETICAL FRAMEWORK OF THE IN-MEDIUM EVOLUTION OF D^0 MESON-TAGGED JETS IN A+A

When a fast parton traverses a hot and dense medium, it will lose its energy by radiating gluons due to multiple scatterings in such a medium. The spectrum of the radiative gluon is calculated from multiple gluon emission theories [16–25]. In this letter, we implement the formalism of the Higher-Twist approach [16–18]:

$$\frac{{\rm d}N}{{\rm d}x{\rm d}k_\perp^2{\rm d}t} = \frac{2\alpha_s C_s P(x)\hat{q}}{\pi k_\perp^4}\sin^2\left(\frac{t-t_i}{2\tau_f}\right)\left(\frac{k_\perp^2}{k_\perp^2+x^2M^2}\right)^4, \quad (2)$$

where x and $k_\perp$ are the energy fraction and transverse momentum of a radiated gluon, respectively, M is the mass of the parent parton, α_s is the strong coupling constant, C_s is the quadratic Casimir in color representation, $P(x)$ is the vacuum splitting function [39], the jet transport coefficient $\hat{q} \propto \hat{q}_0(T/T_0)^3$ [20], and the gluon formation time is $\tau_f = 2Ex(1-x)/(k_\perp^2 + x^2M^2)$.

The dead-cone effect manifests itself in the last quartic term of Eq. (2). One can easily rewrite this term as $(1+\theta_0^2/\theta^2)^{-4}$, with the relations $\theta_0 = M/E$ and $k_\perp = xE\theta$. The radiative gluon spectrum for massive quarks will be largely suppressed when the radiation angle $\theta < \theta_0$. It is very interesting to investigate how the detailed effect manifests itself in the QCD medium-modified emission angle distributions of heavy quark-initiated splittings.

Taking advantage of the previous study on p+p collisions, we compute the same charm quark-initiated and light parton-initiated splittings to demonstrate the possible dead-cone effect in A+A collisions. The Simulating Heavy quark Energy Loss with Langevin equations (SHELL) model [40–43] is employed to describe the in-medium evolution of the heavy parton considering both collisional and radiative energy loss mechanisms. The SHELL model has already been utilized to predict the number of heavy flavor jet-related observables [3, 33, 44]. It is built on the framework of the modified Langevin equations describing the propagation of heavy quarks [40, 42, 43, 45, 46]:

$$\Delta\vec{x}(t) = \frac{\vec{p}(t)}{E}\Delta t\,, \quad (3)$$

$$\Delta\vec{p}(t) = -\Gamma(p,T)\vec{p}\Delta t + \vec{\xi}(t)\sqrt{\Delta t} - \vec{p}_g(t)\,, \quad (4)$$

where Δt is the time interval between each Monte Carlo simulation step, drag coefficient Γ is constrained by the fluctuation-dissipation relation [47] with momentum diffusion coefficient κ, $\Gamma = \kappa/2ET = T/D_sE$, and $D_s = 4/(2\pi T)$. D_s is the spacial diffusion coefficient. The thermal stochastic term $\vec{\xi}(t)$, which gives random kicks on the heavy quarks from thermal quasi-particles in QGP, obeys the Gaussian distribution $\langle\xi^i(t)\xi^j(t')\rangle = \kappa\delta^{ij}\delta(t-t')$. The last term in Eq. (4) is the momentum recoil due to the medium-induced gluon radiation, which is implemented with the higher-twist approach in Eq. (2). During each time interval, the in-medium gluon radiation probability, which is also calculated from Eq. (2) and assumed to obey the Poisson distribution, is implemented to decide whether radiation occurs during a Langevin evolution time interval, $P(n) = \lambda^n {\rm e}^{-\lambda}/n!$, which represents the prob-

ability $P(n)$ of radiating n gluons during time interval Δt. λ is the mean value of n and can be calculated by integrating Eq. (2):

$$\lambda(t,\Delta t)=\Delta t\int \mathrm{d}x\mathrm{d}k_{\perp}^{2}\frac{\mathrm{d}N}{\mathrm{d}x\mathrm{d}k_{\perp}^{2}\mathrm{d}t}. \tag{5}$$

If radiation occurs, the number of radiated gluons is determined by $P(n)$, and the four-momentum of each radiated gluon can be updated in Eq. (2), *i.e.*, the last term $\vec{p}_g$ of Eq. (4) in each time interval Δt. The simulation of a parton propagating in the hot and dense medium will continue evolving as described above until the temperature of the medium decreases to $T_c = 165$ MeV. The space-time evolution of the QCD medium is provided by a (3+1)D viscous hydrodynamic model, CLVisc [48]. An energy cutoff of $\omega_0 \geq \mu_D = \sqrt{4\pi\alpha_s}T$ is set to maintain the fluctuation-dissipation relation for heavy quarks, and the initial parton positions are provided by Glauber Monte Carlo [49]. The value of $\hat{q}_0 = 1.5\ \mathrm{GeV}^2/\mathrm{fm}$ is extracted from χ^2 calculations in final-state hadron productions in Pb + Pb collisions at $\sqrt{s}$ = 5.02 TeV [50, 51]. The value $D_s(2\pi T) = 4$ extracted from χ^2 calculations in D meson R_{AA} between theoretical calculations and experimental data [52−55] is consistent with $D_s(2\pi T) = 3.7 \sim 7$ obtained from Lattice QCD calculations [56, 57].

The radiative energy loss of light partons is considered the same as that of heavy quarks in the same Langevin time step. To simulate the collisional energy loss of the light partons, a Hard Thermal Loop (HTL) formula [58] was adopted in this work: $\mathrm{d}E^{\mathrm{coll}}/\mathrm{d}t = \frac{\alpha_s C_s \mu_D^2}{2}\ln\frac{\sqrt{ET}}{\mu_D}$. When all partons stop their propagation in the QGP medium and fragment into hadrons, we first construct strings using the colorless method developed by the JETSCAPE collaboration[59] and then perform hadronization and hadron decays using the PYTHIA Lund string method.

IV. OBSERVATION OF THE DEAD-CONE IN *A+A* COLLISIONS

In Fig. 2, we calculate the splitting angle distributions normalized to the number of jets for both D^0 meson-tagged jets and inclusive jets in Pb+Pb collisions at $\sqrt{s} = 5.02$ TeV displayed in the upper panels, shown as solid lines in different colors. They are presented in the same three energy intervals of the radiators as in p+p; furthermore, the results for light flavor initiated jets are also plotted as no-quark mass (dead-cone) reference. Then, the ratio of these two distributions is expected to help expose the possible suppression in the dead-cone region of splitting angle θ. By comparing the $R^{AA}(\theta)$ distributions as a function of $\ln(1/\theta)$ with the no-quark mass (dead-cone) limit at the different radiators' energy intervals, we find that such suppression begins to vanish as the energy of the radiator increases. However, there will also be a mass effect in the collisional energy loss mechanism, which is not expected to be affected by such suppression in the dead-cone region of the splitting angle. It is important to investigate such pollution to isolate the observation of the dead-cone effect implemented in the radiative energy loss mechanism.

To verify that such suppression is truly due to the dead-cone effect embedded in the formalism of the higher-twist approach that describes the radiative energy loss due to multiple scattering, the upper panels of Fig. 3 compute the splitting angle distributions of the D^0 meson-tagged jets normalized to the number of jets in Pb+Pb collisions at $\sqrt{s} = 5.02$ TeV. Also, the A+A/p+p ratios

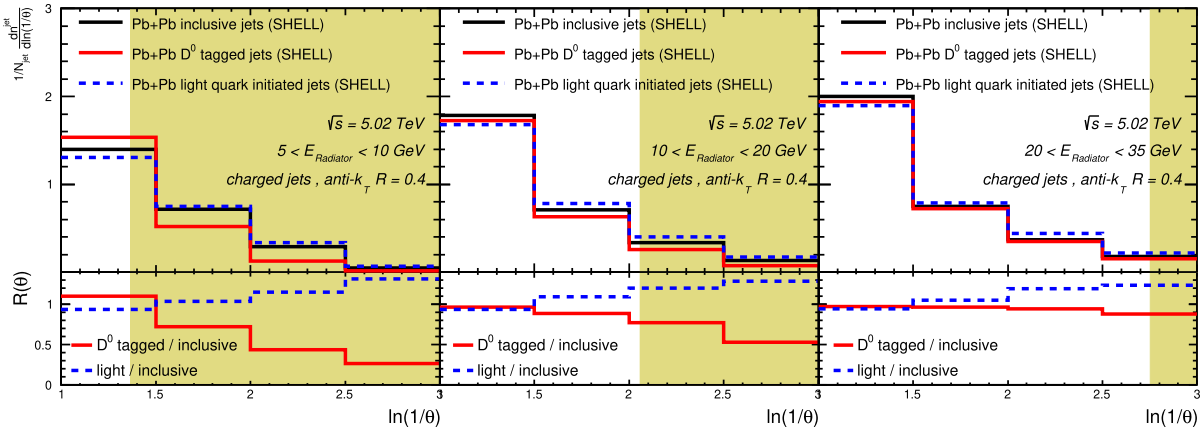

Fig. 2. (color online) Splitting angle distributions for D^0 meson-tagged jets, inclusive jets, and light quark jets normalized to the number of jets in Pb+Pb collisions at $\sqrt{s} = 5.02$ TeV (upper plots), as well as the D^0 meson-tagged jets/inclusive jet (light quark jets/inclusive jets) ratios (bottom plots) calculated for three energy intervals of the radiators: $5 < E_{\mathrm{Radiator}} < 10$ GeV (left panel), $10 < E_{\mathrm{Radiator}} < 20$ GeV (middle panel), and $20 < E_{\mathrm{Radiator}} < 35$ GeV (right panel). The shaded areas correspond to the angles at which the radiation is suppressed due to the dead-cone effect.

from separated contributions for collisional and radiative energy losses in the bottom panel are shown by the dashed and solid lines, respectively. We find that the radiative energy loss contribution will lead the distribution in Pb+Pb to shift to a larger θ region than p+p for all three energy intervals of radiators. However, the collisional energy loss contribution will barely affect the $\ln(1/\theta)$ distributions for the D^0 meson-tagged jets in p+p. We can conclude that the collisional energy loss mechanism has a negligible impact on the medium modification to the emission angle distribution of the charm-quark-initiated splittings for D^0 meson-tagged jets. Only the radiative energy loss contribution will be responsible for the medium modification to the $\ln(1/\theta)$ distributions for the D^0 meson-tagged jets. Therefore, $R_{AA}(\theta)$ can be computed using the same iterative jet declustering techniques applied in p+p and then measured experimentally. It also can be proposed to disclose the measurement of the dead-cone effect of the medium-induced radiation in jet quenching. This will further help constrain the radiative energy loss description of jet quenching models and help gain more understanding of the in-medium evolution of the jet shower.

Figure 4 also computes the splitting angle distributions for inclusive jets normalized to the number of jets in Pb+Pb collisions at $\sqrt{s} = 5.02$ TeV, as well as the A+A/p+p ratios for all three energy intervals of the radiators. We find that both in the light and heavy flavor cases, the splitting angle distributions are always shifting to larger θ (small $\ln(1/\theta)$) due to jet quenching. We can easily summarize that the medium-induced radiation will broaden the splittings for heavy- and light-initiated partons compared to the case in p+p.

When taking a closer look at the values of heavy/light ratios demonstrated in Fig. 1 and Fig. 2, unlike what we observed in A+A/p+p ratios discussed above, we find that

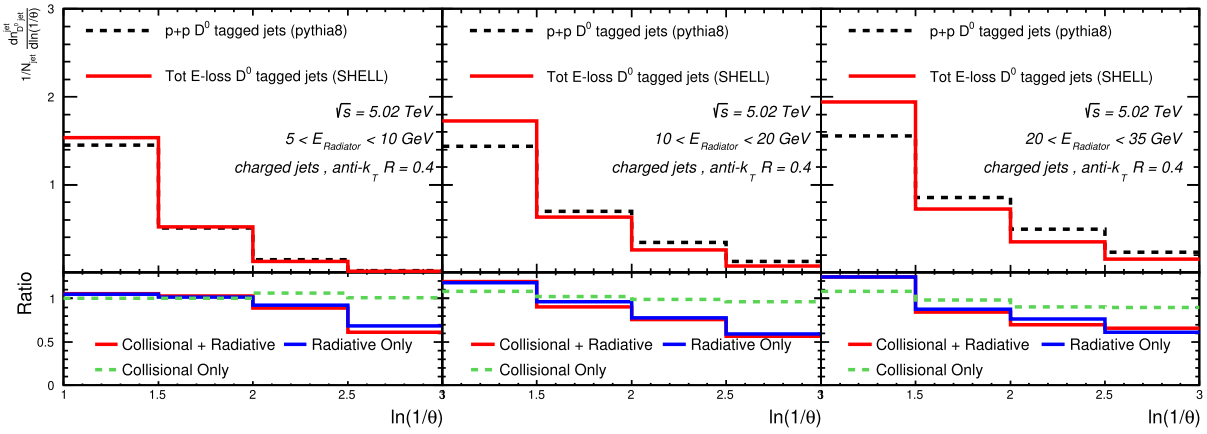

Fig. 3. (color online) Splitting angle distributions of the D^0 meson-tagged jets normalized to the number of jets in p+p and A+A collisions at $\sqrt{s} = 5.02$ TeV (upper plots), as well as their A+A/p+p ratios (bottom plots) calculated for three energy intervals of the radiators: $5 < E_{\rm Radiator} < 10$ GeV (left panel), $10 < E_{\rm Radiator} < 20$ GeV (middle panel), and $20 < E_{\rm Radiator} < 35$ GeV (right panel). Also, the contributions from the radiative and collisional energy losses in A+A collisions are presented accordingly.

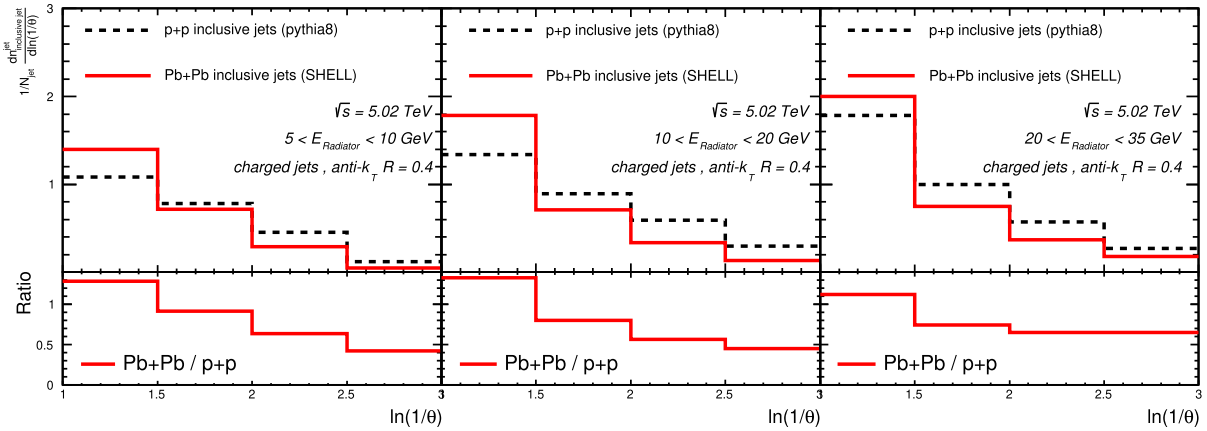

Fig. 4. (color online) Splitting angle distributions of the inclusive jets normalized to the number of jets in p+p (dash lines) and A+A (solid lines) collisions at $\sqrt{s} = 5.02$ TeV (upper plots), as well as their A+A/p+p ratios (bottom plots) calculated for three energy intervals of the radiators: $5 < E_{\rm Radiator} < 10$ GeV (middle panel), $10 < E_{\rm Radiator} < 20$ GeV (right panel), and $20 < E_{\rm Radiator} < 35$ GeV (left panel).

the number of jets normalized emission angle distribution ratios in p+p are smaller than 1 at all the investigated θ regions at $20 < E_{\rm Radiator} < 35$ GeV, in the case of A+A and at $10 < E_{\rm Radiator} < 20$ GeV and $20 < E_{\rm Radiator} < 35$ GeV. It is not easy to understand such suppression at all investigated regions. To address this concern, we systematically calculate the averaged values of splitting angles per jet in D^0-meson (inclusive) jets in p+p and Pb+Pb at $\sqrt{s} = 5.02$ TeV, as demonstrated in Table 1, for each energy interval. Indeed, we find the averaged values for D^0 jets are smaller than the inclusive ones both in p+p and A+A in $10 < E_{\rm Radiator} < 20$ GeV and $20 < E_{\rm Radiator} < 35$ GeV, which is consistent with what we observed in the heavy/light ratios as functions of θ, highlighting an important caveat.

We believe that the number of splittings along the tracked prong in the investigated jets needs to be considered and further investigated. In Table 2, averaged splitting angles per splitting are calculated in D^0-meson (inclusive) jets in p+p and Pb+Pb at $\sqrt{s} = 5.02$ TeV, and the numbers of reconstructed splittings in jets are also provided accordingly. We find that the averaged splitting angles per splitting of the D^0 meson-tagged jets are larger than those of the inclusive jets both in p+p and A+A, and the averaged splitting angles per splitting in A+A are also larger than their counterparts in p+p. We can also find the numbers of splittings in D^0 meson-tagged jets in each energy interval is always smaller than that in inclusive jets. All calculations were cross-checked with LBT calculations [60, 61], the values of the calculation results in A+A collisions using LBT are 1%−2% larger than those using SHELL. Then, the probability of heavy quark-emitting gluons at a smaller angle is largely suppressed due to the dead-cone effect. This lead to the emissions being distributed at a larger angle. However, the possibility of emitting such gluons is suppressed due to this mass effect governed by the dead-cone term in Eq. (2).

Table 1. Averaged splitting angles in jets for D^0 meson-tagged and inclusive jets calculated in both p+p and Pb+Pb collisions at $\sqrt{s} = 5.02$ TeV at three energy intervals: $5 < E_{\rm Radiator} < 10$ GeV, $10 < E_{\rm Radiator} < 20$ GeV, and $20 < E_{\rm Radiator} < 35$ GeV respectively.

$E_{\rm Radiator}$	Inclusive jets	D^0 jets	
	$\langle\theta\rangle_{\rm jets}$	$\langle\theta\rangle_{\rm jets}$	
5 – 10 GeV	0.31	0.34	pp
	0.36	0.36	AA
10 – 20 GeV	0.40	0.37	pp
	0.45	0.42	AA
20 – 35 GeV	0.47	0.42	pp
	0.49	0.47	AA

Table 2. Averaged splitting angles per splitting for D^0 meson-tagged and inclusive jets are calculated in both p+p and Pb+Pb collisions at $\sqrt{s} = 5.02$ TeV at three energy intervals: $5 < E_{\rm Radiator} < 10$ GeV, $10 < E_{\rm Radiator} < 20$ GeV, and $20 < E_{\rm Radiator} < 35$ GeV. The numbers of splittings in jets are also provided accordingly.

$E_{\rm Radiator}$	Inclusive jets		D^0 jets		
	$\langle\theta\rangle_{\rm spl}$	$N_{\rm spl}$	$\langle\theta\rangle_{\rm spl}$	$N_{\rm spl}$	
5 – 10 GeV	0.227	1.358	0.277	1.233	pp
	0.256	1.405	0.280	1.280	AA
10 – 20 GeV	0.220	1.810	0.244	1.510	pp
	0.254	1.757	0.263	1.600	AA
20 – 35 GeV	0.232	2.040	0.232	1.822	pp
	0.249	1.977	0.251	1.860	AA

V. CONCLUSIONS

Using the SHELL model, we calculated the emission angle distribution of charm-quark-initiated and light parton-initiated splittings, both in p+p and Pb+Pb at $\sqrt{s} = 5.02$ TeV. First, we validated our vacuum reference calculation by comparing it to the ALICE p+p dead cone results. We then reported the results of the full simulation, which includes medium-induced radiation as well as collisional energy loss. We found that the splitting angle distributions get broader in Pb+Pb relative to p+p due to medium-induced radiation both for D^0 meson-tagged and inclusive jets. The mass effect will also induce the splitting angle distributions to become broader both in p+p and Pb+Pb. Still, we observed a dead-cone signal in Pb+Pb: a strong suppression of small-angle splittings for D^0 meson-tagged jets relative to inclusive ones. We also found that the collisional energy loss does not induce suppression of small splitting angles for D^0 meson-tagged jets. The scenario of dead-cone effect is that the survived splitting angle of heavy flavor-initiated splitting is distributed at a larger angle; however, the possibility of such emission will be reduced.

ACKNOWLEDGMENTS

The authors would like to thank X Peng for helpful discussions.

References

[1] S. Marzani, G. Soyez, and M. Spannowsky, Lecture Note in Physics **958**, 252 (2019)

[2] Y. L. Dokshitzer, V. A. Khoze, and S. I. Troian, J. Phys. G **17**, 1602 (1991)

[3] A. M. Sirunyan *et al*. (CMS), Phys. Rev. Lett. **125**, 102001 (2020), arXiv: 1911.01461
[4] P. Abreu *et al*. (DELPHI), Phys. Lett. B **479**, 118 (2000), [Erratum: Phys. Lett. B 492, 398 (2000)]
[5] K. Abe *et al*. (SLD), Phys. Rev. Lett. **84**, 4300 (2000), arXiv: hep-ex/9912058
[6] J. Llorente and J. Cantero, Nucl. Phys. B **889**, 401 (2014), arXiv: 1407.8001
[7] C. Frye, A. J. Larkoski, J. Thaler *et al*., JHEP **09**, 083 (2017), arXiv: 1704.06266
[8] F. A. Dreyer, G. P. Salam, and G. Soyez, JHEP **12**, 064 (2018), arXiv: 1807.04758
[9] L. Cunqueiro and M. Płoskoń, Phys. Rev. D **99**, 074027 (2019), arXiv: 1812.00102
[10] S. Acharya *et al*. (ALICE), Nature **605**, 440 (2022a), arXiv: 2106.05713
[11] X.-N. Wang and M. Gyulassy, Phys. Rev. Lett. **68**, 1480 (1992)
[12] M. Gyulassy, I. Vitev, X.-N. Wang *et al*., arXiv: nucl-th/0302077
[13] G.-Y. Qin and X.-N. Wang, Int. J. Mod. Phys. E **24**, 1530014 (2015), arXiv: 1511.00790
[14] J. Viinikainen (CMS), Acta Phys. Polon. Supp. **16**, 59 (2023)
[15] J. F. Grosse-Oetringhaus (ALICE), arXiv: 1109.6208
[16] X.-F. Guo and X.-N. Wang, Phys. Rev. Lett. **85**, 3591 (2000), arXiv: hep-ph/0005044
[17] B.-W. Zhang and X.-N. Wang, Nucl. Phys. A **720**, 429 (2003), arXiv: hep-ph/0301195
[18] B.-W. Zhang, E. Wang, and X.-N. Wan, Phys. Rev. Lett. **93**, 072301 (2004), arXiv: nucl-th/0309040
[19] A. Majumder, Phys. Rev. D **85**, 014023 (2012), arXiv: 0912.2987
[20] X.-F. Chen, C. Greiner, E. Wang *et al*., Phys. Rev. C **81**, 064908 (2010), arXiv: 1002.1165
[21] X.-F. Chen, T. Hirano, E. Wang *et al*., Phys. Rev. C **84**, 034902 (2011), arXiv: 1102.5614
[22] I. Vitev, M. Gyulassy, and P. Levai, Acta Phys. Hung. A **17**, 237 (2003), arXiv: nucl-th/0204019
[23] P. B. Arnold, G. D. Moore, and L. G. Yaffe, JHEP **11**, 001 (2000), arXiv: hep-ph/0010177
[24] P. B. Arnold, G. D. Moore, and L. G. Yaffe, JHEP **05**, 051 (2003), arXiv: hep-ph/0302165
[25] R. Baier, D. Schiff, and B. G. Zakharov, Ann. Rev. Nucl. Part. Sci. **50**, 37 (2000), arXiv: hep-ph/0002198
[26] Y. L. Dokshitzer and D. E. Kharzeev, Phys. Lett. B **519**, 199 (2001), arXiv: hep-ph/0106202
[27] N. Armesto, C. A. Salgado, and U. A. Wiedemann, Phys. Rev. D **69**, 114003 (2004), arXiv: hep-ph/0312106
[28] B.-W. Zhang, E.-K. Wang, and X.-N. Wang, Nucl. Phys. A **757**, 493 (2005), arXiv: hep-ph/0412060
[29] S. S. Adler *et al*. (PHENIX), Phys. Rev. Lett. **94**, 082301 (2005), arXiv: nucl-ex/0409028
[30] B. I. Abelev *et al*. (STAR), Phys. Rev. Lett. **98**, 192301 (2007), [Erratum: Phys. Rev. Lett. 106, 159902 (2011)]
[31] B. Abelev *et al*. (ALICE), JHEP **09**, 112 (2012), arXiv: 1203.2160
[32] V. Khachatryan *et al*. (CMS), Eur. Phys. J. C **77**, 252 (2017), arXiv: 1610.00613
[33] G. Aad (ATLAS), Eur. Phys. J. C **83**, 438 (2023)
[34] T. Sjostrand, S. Mrenna, and P. Z. Skands, Comput. Phys. Commun. **178**, 852 (2008), arXiv: 0710.3820
[35] M. Cacciari, G. P. Salam, and G. Soyez, JHEP **04**, 063 (2008), arXiv: 0802.1189
[36] M. Cacciari, G. P. Salam, and G. Soyez, Eur. Phys. J. C **72**, 1896 (2012), arXiv: 1111.6097
[37] Y. L. Dokshitzer, G. Leder, S. Moretti *et al*., JHEP **08**, 001 (1997), arXiv: hep-ph/9707323
[38] A. Lifson, G. P. Salam, and G. Soyez, JHEP **10**, 170 (2020), arXiv: 2007.06578
[39] W.-T. Deng and X.-N. Wang, Phys. Rev. C **81**, 024902 (2010), arXiv: 0910.3403
[40] W. Dai, S. Wang, S.-L. Zhang *et al*., Chin. Phys. C **44**, 104105 (2020), arXiv: 1806.06332
[41] S. Wang, W. Dai, B.-W. Zhang *et al*., Chin. Phys. C **45**, 064105 (2021a), arXiv: 2012.13935
[42] S. Wang, W. Dai, J. Yan *et al*., Nucl. Phys. A **1005**, 121787 (2021b), arXiv: 2001.11660
[43] S. Wang, W. Dai, B.-W. Zhang *et al*., arXiv: 2005.07018
[44] S. Acharya *et al*. (ALICE), JHEP **05**, 061 (2022b), arXiv: 2107.11303
[45] S. Cao, G.-Y. Qin, and S. A. Bass, Phys. Rev. C **88**, 044907 (2013), arXiv: 1308.0617
[46] S. Wang, W. Dai, B.-W. Zhang *et al*., Eur. Phys. J. C **79**, 789 (2019), arXiv: 1906.01499
[47] M. He, H. van Hees, P. B. Gossiaux *et al*., Phys. Rev. E **88**, 032138 (2013), arXiv: 1305.1425
[48] L. Pang, Q. Wang, and X.-N. Wang, Phys. Rev. C **86**, 024911 (2012), arXiv: 1205.5019
[49] M. L. Miller, K. Reygers, S. J. Sanders *et al*., Ann. Rev. Nucl. Part. Sci. **57**, 205 (2007), arXiv: nucl-ex/0701025
[50] G.-Y. Ma, W. Dai, B.-W. Zhang *et al*., Eur. Phys. J. C **79**, 518 (2019), arXiv: 1812.02033
[51] Q. Zhang, W. Dai, L. Wang *et al*., arXiv: 2203.10742
[52] L. Adamczyk *et al*. (STAR), Phys. Rev. Lett. **113**, 142301 (2007), [Erratum: Phys. Rev. Lett. 121, 229901 (2018)], arXiv: 1404.6185
[53] G. Xie (STAR), Nucl. Phys. A **956**, 473 (2016), arXiv: 1601.00695
[54] A. M. Sirunyan *et al*. (CMS), Phys. Lett. B **782**, 474 (2018), arXiv: 1708.04962
[55] S. Acharya *et al*. (ALICE), JHEP **10**, 174 (2018), arXiv: 1804.09083
[56] A. Francis, O. Kaczmarek, M. Laine *et al*., Phys. Rev. D **92**, 116003 (2015), arXiv: 1508.04543
[57] N. Brambilla, V. Leino, P. Petreczky *et al*., Phys. Rev. D **102**, 074503 (2020), arXiv: 2007.10078
[58] R. B. Neufeld, Phys. Rev. D **83**, 065012 (2011), arXiv: 1011.4979
[59] J. H. Putschke *et al*., arXiv: 1903.07706
[60] Y. He, T. Luo, X.-N. Wang *et al*., Phys. Rev. C **91**, 054908 (2015), [Erratum: Phys. Rev. C 97, 019902 (2018)], arXiv: 1503.03313
[61] S. Cao, T. Luo, G.-Y. Qin *et al*., Phys. Rev. C **94**, 014909 (2016), arXiv: 1605.06447